

Range Membership Inference Attacks

Jiashu Tao[†], and Reza Shokri[†]

[†] National University of Singapore, {jiashut, reza}@comp.nus.edu.sg

Abstract

Machine learning models can leak private information about their training data, but the standard methods to measure this risk, based on membership inference attacks (MIAs), have a major limitation. They only check if a given data point *exactly* matches a training point, neglecting the potential of similar or partially overlapping data revealing the same private information. To address this issue, we introduce the class of range membership inference attacks (RaMIAs), testing if the model was trained on any data in a specified range (defined based on the semantics of privacy). We formulate the RaMIAs game and design a principled statistical test for its composite hypotheses. We show that RaMIAs can capture privacy loss more accurately and comprehensively than MIAs on various types of data, such as tabular, image, and language. RaMIA paves the way for a more comprehensive and meaningful privacy auditing of machine learning algorithms.

1 Introduction

Machine learning models are prone to training data memorization [14, 15, 27, 42, 24]. It is also a known fact that the outstanding predictive performance of machine learning models on long-tailed data distributions often comes at the expense of blatant memorization of certain data points [15, 3, 30, 16]. In simple words, memorization is the phenomenon that models behave differently on training points, compared to other points. The memorization can lead to significant privacy risks as adversaries can infer private information about the training data from only having black box access to models.

To quantify the privacy risk of machine learning models, a privacy notion needs to be agreed upon first. The reigning privacy notion is defined by *membership* information. Membership information of a data point is binary, but this single bit of information carries huge privacy implications. Being able to infer membership information opens up the possibility of conducting data *reconstruction* attack [37, 17, 4, 29], where the reconstruction attack inspects the membership of plausible data points to recover the training set. The de-facto way to audit the privacy risk according to this privacy notion is to conduct membership inference attacks (MIAs) [40], where an adversary aims to predict whether a given query data is part of the training set of the target model. The more powerful the membership inference attack is, the higher the privacy risk the target model bears.

Membership inference attacks provide a lower bound of the true privacy risk of a model, so improving the attack performance also means tightening the bound of privacy risk estimation. So far, the community has put much effort into improving the power of membership inference attacks by crafting better membership signals and constructing better statistical tests [39, 40, 36, 45, 5, 48]. While these have been useful for the betterment of privacy auditing, they have ignored the fundamental drawback of membership inference attacks as a practical privacy auditing tool, i.e.,

MIAs assume it is a privacy concern *only if* the adversary can identify the **exact, full version** of the training data. However, if the adversary can identify data points that are similar enough to the training points, it should also be treated as a significant privacy risk, because those points can contain similar levels of private information. For example, two Alice’s photos taken from slightly different angles, or with a different background would contain similar private information about Alice’s face or location. Similar to geometric transformations in images, small perturbations or rephrasing in textual data also affect little in the sensitivity of the information conveyed [13]. This oversight means private information leakage beyond exact matches of training data is currently ignored and the contemporary privacy auditing tools might produce overly optimistic results.

Besides, focusing on exact membership inference attacks renders them incapable of handling queries with *missing values*. This is another major limitation of MIAs, as data records with the same sensitive features and a few missing non-private features could carry a similar level of private information as the full data records. Imagine the case where an adversary can infer that an Asian person of age 25, identification number 123456 is in an HIV patients dataset, there is no need to identify or collect the exact values of the rest of the features, because the adversary is already able to pinpoint who has HIV from the given subset of key features. Even if the key identifiers are missing and unknown, it is still a grave privacy threat if the attacker can infer the rest of the features from the subset of known features that often contain quasi-identifiers, which has been extensively studied in the failure of *k-anonymity* as a privacy-preserving measure [38], where the attacker can reconstruct and identify training data with certain features masked. With existing inference attacks, there are two types of approaches to work with incomplete data. The first approach is to impute the missing features before performing membership inference attacks. However, if we simply make up the missing values or pass noisy data to the membership inference attack, the attack is expected to output “not a member,” since the chance of us coming up with the right values is extremely slim. If we use attribute inference [20] to help fill in the missing features, the imputed data may have inflated membership scores even if they are non-members, leading to a higher false positive rate. Therefore, existing MIA-based privacy auditing frameworks does not provide a natural solution to quantifying privacy leakage with missing features. The second approach that works with incomplete data is property inference [41, 1, 8, 9, 46], but it aims to extract statistical information about the features instead of testing membership information of data records. Hence, none of the existing inference attack frameworks can reliably quantify privacy leakage with incomplete data entries.

We argue that privacy quantification should not be point-based, because a small neighborhood around training points, defined based on a distance function out of the semantics of privacy, also contains similar private information. Hence, in this paper, we are proposing a new inference attack framework called **range membership inference attacks** (RaMIAs) to better capture the notion of privacy. Instead of using point queries and testing for exact matches, range membership inference attacks use range queries that cover a set of points. The goal of range membership inference attacks is to infer if the given **range query** contains any training point. In this paper, we denote the “neighborhood” as the “range”, and its corresponding distance function as the “range function”.

Range membership inference attacks extend the formulation of membership inference attacks. We adapt the original inference game formulation to reflect the change to range queries in RaMIAs. This extended formulation produces composite hypotheses in the likelihood ratio tests, which are the standard and best attack techniques in MIAs [39, 45, 5, 48]. Our method is based



(a) MIA Score=2.99



(b) MIA Score=2e-15

Judging Error Led to Hamm’s Gold ATHENS, Greece - Paul Hamm thought his fantastic finish was too good to be true. Maybe he was **right...**

Judging Error Led to Hamm’s Gold ATHENS, Greece - Paul Hamm thought his fantastic finish was too good to be true. Maybe he was **?**

(c) MIA Score=1.8 and 1.0

Figure 1: Examples of similar data with drastically different MIA scores. MIA would classify one of them as member, but the other as non-member. The dog image is from the CIFAR-10 dataset, while the text data is from AG News. The image classifier is not trained with horizontal flipping augmentation.

on standard statistical methods for composite hypothesis testing, namely generalized likelihood ratio tests (GLRTs) and Bayes factors. We show that RaMIAs can provide a more comprehensive notion of privacy by detecting private information leakage from the vicinity of training data when MIAs underestimate such privacy risk. Specifically, we observe a simple flipping can cause the membership score to decrease from very high to 0 (Figure 1), and the overall AUC can drop 20% if we test image classifiers with horizontally flipped images (Figure 2c). This is actually the expected behavior of MIAs since the transformed training data are non-members by definition. RaMIA, implemented with our simple attack algorithm (Sec 4), surpasses MIA by at least 5% on image datasets (Fig 3b, 3c), providing better privacy auditing at the cost of as few as 15 samples, which is insignificant compared to the dimensionality of the data space.

In this paper, we emphasize the motivation and formulation of our newly proposed attack framework, RaMIA. As a proof-of-concept, we implement RaMIA with a simple attack strategy and experiment on tabular, image and text datasets, where RaMIA unanimously outperforms MIA. Additionally, our attack can also be potentially used in the pioneering membership inference and data extraction attacks on generative models [4, 44, 7], where the current evaluation requires finding the closest training image for all candidate data and computing their distances. By setting the distance function as the range function and conducting RaMIAs, we can evaluate the attacks more systematically.

2 Preliminaries

2.1 Membership inference attacks

The membership inference attack (MIA) [40] is a type of inference attack against machine learning models to infer whether a given data sample is part of the model’s training set. Mathematically, given a model f and a query point \mathbf{x} , the MIA aims to output 1 if \mathbf{x} is a training point, and 0 otherwise. There are various methods to construct and conduct the attack, and it is still an active research direction that sees more powerful attacks being developed. Shokri et al. [40] use a shadow model-based approach where shadow models are trained on known training sets in

similar ways to the target model. Confidence values of the training and test data on the shadow models are computed, which are then used as benchmarks in testing. However, the high cost and strong assumption of knowing the target model’s training details make the attack often infeasible. Yeom et al. [46] use model loss as a signal and threshold it, scraping the need for shadow models. Then MIA is formulated as an inference game (See Sec 3.1.1). Researchers turn to the principled approach to solve the game via likelihood ratio tests [39, 5, 45, 48]. Carlini et al. [5] and Ye et al. [45] propose reference-model based approaches, where target signals are compared to those obtained on reference models to obtain the likelihood ratio. To further boost the attack power, Zarifzadeh et al. [48] assumes the attacker has access to a pool of population data so that the likelihood ratio from reference-based attacks can be calibrated on ratios obtained on (non-member) population data.

Membership inference attacks with augmentations Recent attacks [5, 48] find extra attack performance on image data from augmenting the test queries with *train-time* augmentations, as these augmented training images could have been seen by the model during training. However, this assumes that the attacker knows the exact train-time augmentations in advance, and is able to sample from them. Augmenting training images with non train-time augmentations is not considered and allowed for valid reasons: those augmented images would be non-members in the current privacy notion based on membership inference, and testing them as members would violate the current privacy notion.

2.2 Range queries

If we make a connection to the field of databases, the existing membership inference attack operates on *point queries* or *exact match queries*. That is, each query to the membership inference attack only contains one data point and the attack only concerns if this very point is in the training set. On the other hand, range query, which is also a common querying operation in database systems, wants to retrieve all data points that fall into the “range”. The most fundamental difference to point query is that the retrieved result often contains multiple data points instead of a single one. Our proposed attack, the range membership inference attack, operates with range queries.

3 From MIA to RaMIA

Membership inference attacks are often formulated as an inference game [46, 21, 45, 5, 48] between a *challenger* and an *adversary*. In this section, we will walk through how we come up with RaMIA from MIA.

3.1 Membership inference attacks

In membership inference attacks, the goal is to identify if a given point is part of the training set.

3.1.1 Membership inference game

Definition 1 (*Membership Inference Game* [45, 46]) *Let π be the data distribution, and let \mathcal{T} be the training algorithm.*

1. *The challenger samples a training dataset $D \xleftarrow{s_D} \pi$, and trains a model $\theta \leftarrow \mathcal{T}(D)$.*

2. The challenger samples a data record $z_0 \xleftarrow{s_{z_0}} \pi$ from the data distribution, and a training data record $z_1 \xleftarrow{s_{z_1}} D$.
3. The challenger flips a fair coin to get the bit $b \in \{0, 1\}$, and sends the target model θ and data record z_b to the adversary.
4. The adversary gets access to the data distribution π and access to the target model, and outputs a bit $\hat{b} \leftarrow \mathcal{A}(\theta, z_b)$.
5. If $\hat{b} = b$, output 1 (success). Otherwise, output 0.

3.1.2 Evaluation of MIA

Evaluation is done with a set of training and test points. True positive rate (TPR) and false positive rate (FPR) are computed by sweeping over all possible threshold values. By plotting the receiver operating characteristic curve (ROC), the power of an attack strategy can be represented by the area under the curve (AUC). A clueless adversary who can only randomly guess the membership labels is expected to get an AUC of 0.5. For stronger adversaries, they predict membership more accurately at each error level. Hence, they would achieve higher TPR at each FPR, and get a higher AUC.

3.1.3 Intrinsic limitation of MIA as a Privacy Auditing Framework

MIA are intrinsically incapable of identifying points close to training points, regardless of how similar they are, because these points are, by definition, non-members in the scope of MIA. Hence, there is a huge space of points that contain private information but are deemed non-members in the current privacy auditing framework. In this way, MIA as privacy auditing tools become bad when the queries move away from the original data. Figure 2 shows the MIA under-perform on non-original data. This inspires our formulation of RaMIA, where these points will be classified as "members" for better and more comprehensive privacy auditing.

3.2 Range membership inference attack

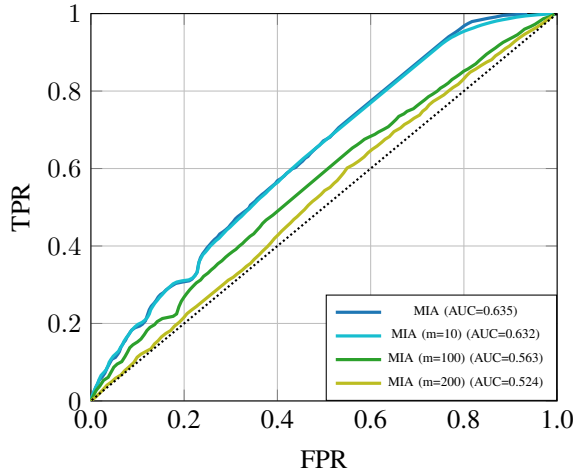
In range membership inference attacks, the goal is to identify if a given *range* contains any training point.

3.2.1 Range membership inference game

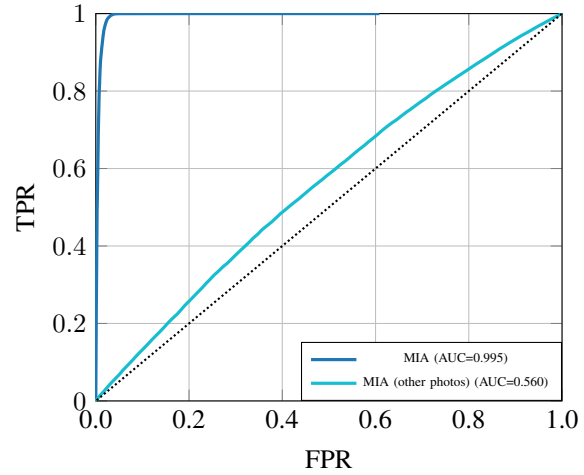
Here we define our range membership inference game, modified from the above formulation.

Definition 2 (*Range Membership Inference Game*) *Let π be the data distribution, and let \mathcal{T} be the training algorithm.*

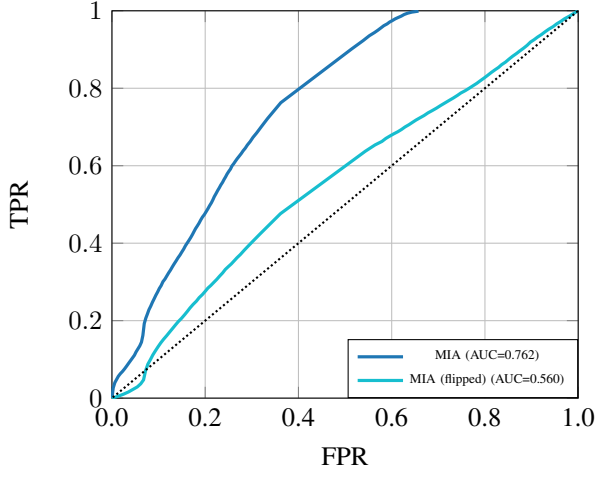
1. The challenger samples a training dataset $D \xleftarrow{s_D} \pi$, and trains a model $\theta \leftarrow \mathcal{T}(D)$.
2. The challenger samples a data record $z_0 \xleftarrow{s_{z_0}} \pi$ from the data distribution, and a training data record $z_1 \xleftarrow{s_{z_1}} D$.
3. The challenger flips a fair coin to get the bit $b \in \{0, 1\}$. If $b = 1$, the challenger samples a range \mathcal{R}_1 containing at least one training point. Otherwise, challenger samples a range \mathcal{R}_0 containing no training points.



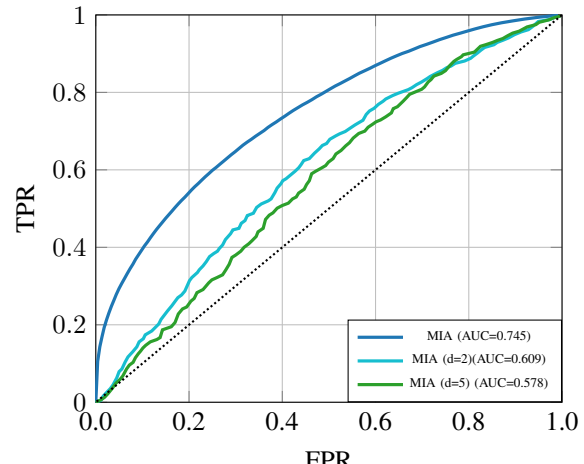
(a) Purchase-100



(b) CelebA



(c) CIFAR-10



(d) AG News

Figure 2: MIA performance gets worse when the query points become further away from the training points. We define points different from training points but carry similar information as members. In 2a, m is the number of missing values. The query is constructed by filling in them with the most likely values. In 2b, the point query changes to photos of the same identity who has at least one photo in the training set. In 2c, the queries are horizontally flipped images. In 2d, d is the Hamming distance to original sentences.

4. The challenger sends the target model θ and the range \mathcal{R}_b to the adversary.
5. The adversary gets access to the data distribution π and access to the target model, and outputs a bit $\hat{b} \leftarrow \mathcal{A}(\theta, \mathcal{R}_b)$.
6. If $\hat{b} = b$, output 1 (success). Otherwise, output 0.

The main difference between the two games is that the *adversary* now receives a range query (Step 4 in Def 2) instead of a point query (Step 3 in Def 1). We assume that the *adversary* is

able to sample a set of points covered by any given range, which effectively means sampling within the range. This is a reasonable assumption because the *adversary* is usually assumed to have the ability to sample from the original data distribution π [40, 45, 48] as specified in the membership inference game formulation. Given a range query and a sampler of π , it is not difficult to sample within the range.

What is a range A range can be defined by a center, which is a point, a radius representing the size of the range, and a distance function which the radius is defined with. We refer to the center as the query center, the radius as the range size, and the distance function as the range function in this paper. One way to visualize a range is to imagine a unit l_2 ball around a point x , replacing the radius and l_2 distance with any arbitrary choice of range sizes and functions. Our framework can cater to any arbitrary range function that is potentially privacy-preserving. It can be spatially based (e.g. l_p distances), transformation based (e.g. geometric transformations), and semantic based (e.g. owner/main features of the data). In the experiment section, we will present results with all of these types of range functions. Note that our attack reduces to user-level inference [31, 23, 27, 11, 10] when the range function is user-based, which means the privacy concern is whether any other data from the same owner are used in training. We will comment on the relations between RaMIA and other existing inference attacks later in the paper.

How to construct a range In Step 3 of the range membership inference game, the details of how the *challenger* samples the ranges are intentionally omitted. This is because the ranges can be constructed around either in-distribution or out-of-distribution data points for both IN and OUT-ranges. The details of how we construct the iIN and OUT-ranges for our experiments are elaborated in Section 5.1.

3.3 Evaluation of RaMIA

Similar to MIAs, we evaluate RaMIA with AUCs. However, the notion of true positives and false positives are different from those defined in MIA, as both are defined on the range level. Specifically, if a range contains at least one training point, it is IN; otherwise, it is OUT. The TPR in RaMIA is the proportion of IN-ranges that are correctly identified by the attacker. On the other hand, the FPR in RaMIA is the proportion of OUT-ranges that yield positive predictions by the attacker. To avoid confusion, we call them (Range) TPR and (Range) FPR.

4 Range membership inference attacks

4.1 (Simple) Hypothesis testing

The standard way to tackle the inference game (Def 1) is to apply statistical hypothesis tests [45, 5]:

$$H_0 : \text{The given } z \text{ is not a training point } (b = 0). \\ H_1 : \text{The given } z \text{ is a training point } (b = 1).$$

The likelihood ratio test (LRT) is then conducted

$$\frac{\mathbb{P}(\theta|H_1)}{\mathbb{P}(\theta|H_0)} \tag{1}$$

This is usually called "simple" hypothesis testing because each H contains a single hypothesis. The scoring function in the membership inference attack can be considered as an approximation of the likelihood function $\mathbb{P}(\cdot)$.

4.2 Composite hypothesis testing

Similar to likelihood ratio tests for membership inference games 4.1, we can also construct two hypotheses for range membership inference game (Def 2):

$$\begin{aligned} H_0 : & \text{None of the points in the given range are} \\ & \text{from the training set. } \forall z \in \mathcal{R}_b : z \notin D. \\ H_1 : & \text{There is at least one point in the given range} \\ & \text{from the training set. } \exists z \in \mathcal{R}_b \text{ s.t. } z \in D. \end{aligned}$$

Since it can be intractable to iterate over all points in a given range \mathcal{R}_b , we use a set of sampled points S in the given range as its proxy. In this way, the two hypotheses are:

$$\begin{aligned} H_0 : & \text{None of the points in the given range are} \\ & \text{from the training set. } \forall z \in S : z \notin D. \\ H_1 : & \text{There is at least one point in the given range} \\ & \text{from the training set. } \exists z \in S \text{ s.t. } z \in D. \end{aligned}$$

The likelihood ratio in this case is still $\frac{\mathbb{P}(\theta|H_1)}{\mathbb{P}(\theta|H_0)}$. However, the alternative hypothesis H_1 is composite because it is a union of multiple hypotheses $\bigcup_{z_i \in S} (z_i \in D)$. Therefore, we need to use statistical methods tailored for composite hypothesis testing. There are two commonly used methods for it: Bayes Factor [22] and Generalized Likelihood Ratio Tests (GLRTs) [43].

GLRT GLRT assumes that the true hypothesis h^* is explicitly listed in the composite hypothesis, which, in our case, means the training point is in the set of samples $\{z_i\}$. In this case, the composite hypothesis can be reduced to a single hypothesis by taking the maximum:

$$\mathbb{P}(\theta|H_1) \Rightarrow \max_{x \in S} \mathbb{P}(\theta|x \in D). \quad (2)$$

Bayes Factor Bayes Factor assumes the hypothesis is a random variable, each with a likelihood value according to a prior distribution. In our case, it means each point z in the range can be sampled with probability determined by the prior data distribution $\mathbb{P}(z)$. To reduce the composite hypothesis to a simple one, Bayes Factor computes the weighted average:

$$\mathbb{P}(\theta|H_1) \Rightarrow \int_{x \in S} \mathbb{P}(\theta|x \in D) \mathbb{P}(x) dx. \quad (3)$$

This can be thought of as taking the expectation of the composite hypothesis or using the most representative hypothesis instead of the maximal (as in GLRT) in the likelihood ratio test.

Why both methods fall short in RaMIA At first look, GLRT might be an intuitive choice, because taking the maximum leads to a two-step strategy: search and test. Searching for the points with the highest membership score is conceptually equivalent to identifying the points that are most likely to be training points, and their membership should be indicative of the ranges’ membership. However, this assumes the true training point is included in every sampled set created by the adversary, which is extremely unlikely. Secondly, this also assumes that we can reliably find the max values in a given range. Since most ranges are large data subspaces, it is very challenging to find the optimal points within the large space. Even if the search space can be navigated, any search algorithm is likely to return local maxima.

To make full use of the Bayes Factor, we need to know the prior distribution, which is also not possible.

A more important issue is that the power of existing statistical methods relies on the absolute correctness of the likelihood values: the larger the likelihood values, the more likely the point is a member. In other words, the largest likelihood values of non-members must be smaller than the smallest likelihood of members. However, membership inference attacks are known to be non-perfect; they are also known to be particularly unreliable on out-of-distribution (OOD) data [48] and can assign them high scores. When the sampling space contains only these data as opposed to real and in-distribution (ID) data, the maximum might not be anything close to true training data, increasing the FPR and lowering the AUC as a result.

4.3 Our approach: Trimmed averages

Given these limitations, in this paper, we propose a simple attack strategy based on Bayes Factor. We first assume every sampled point is of equal probability. Then, to address the unreliability of MIA scores, we use a trimming process based on the type of data in the sampling space. If the data are all naturally ID, we trim the less probable samples and take the average likelihood of the top samples to reduce the influence of non-members and the randomness in the sampling process. On the other hand, if the adversary can only synthesize data within the range instead of sampling from a pool of real data, the top samples are highly likely to be OOD data with high membership scores. Hence, in this case, we want to remove those points from the equation. We then trim the top-scoring samples and take the average of the rest. This gives us the following:

$$\begin{aligned} \text{IP}(\theta|H_1) &= \text{TrimmedAvg}(S, q_s, q_e; \text{IP}) \\ &= \text{Avg}_{x \notin [q_s, q_e]-\text{th quantiles}} \text{IP}(\theta|x \in D), \end{aligned} \tag{4}$$

where S is the sampled set, q_s and q_e mark the start and the end of the quantiles that we want to remove to compute our robust statistics that are one-sided trimmed means. If the sampling space is filled with synthetic data, the chance of the top samples being false positives is high, so we set $q_e = 100$ to remove the largest points. q_s is a hyperparameter that decreases (trim more) as the quality of sampled points gets worse. On the other hand, if the sampling space consists of real points, we set $q_s = 0$ to remove the smallest points in our aggregation. q_e decreases (trim less) as the number of real samples decreases to offset the high variance due to limited samples available. If we do not trim anything, the formulation reduces to Bayes Factor which assigns equal probability to all points.

Note that the optimal hyperparameters may differ across different membership signals (e.g. loss values, LiRA scores), as they exploit different vulnerabilities and expose different training points. However, for fixed model architectures, range functions, data distributions, and sampling methods, these hyperparameters can be determined by reference models, similar to

the offline version of RMIA [48]. Specifically, by randomly choosing a reference model as the temporary target model, we can run RaMIAs using all other reference models while sweeping these hyperparameters in a grid search manner. More details are in Appendix A.

4.4 Range membership inference attack as a framework

The range membership inference attack is a new inference attack framework, not a particular attack algorithm. There are two components in this framework: a sampler and a membership tester, both of which are necessary to compute the range membership score formulated in Eqn 4. The sampler $\text{Sampler}(\mathcal{R}) : S \rightarrow X$ returns samples within the given range. The membership tester $\text{MIA}(x)$ is a (point-query) membership inference algorithm that outputs a membership score, which can be used to approximate $\text{IP}(\theta|x)$. Any existing MIA algorithm can be plugged in as RaMIA’s membership testing backbone. Similar to MIAs, the key to using RaMIA as a privacy auditing tool is to compute the range membership score. Our framework can adopt any existing membership scoring function $\text{MIA}(x)$ to compute RaMIA(\mathcal{R}). Below, we outline the attack with our attack strategy described above:

Algorithm 1 Computing range membership scores

Require: Input range \mathcal{R} , sampler $\text{Sample}(\cdot)$, target model θ , membership scoring function $\text{MIA}(\cdot)$.

- 1: Sample an attack set: $S \xleftarrow{n} \text{Sample}(\mathcal{R})$;
- 2: **if** samples are real and ID **then**
- 3: Set $q_s = 0$, and set q_e by sweeping on reference models;
- 4: **else**
- 5: Set $q_e = 100$, and set q_s by sweeping on reference models.
- 6: **end if**
- 7: $\text{RaMIA}(\mathcal{R}; \theta) = \text{TrimmedAvg}(S, q_s, q_e; \text{MIA})$

5 Experiments

Since the purpose of this paper is to introduce a new concept and framework, the goal of the experiments section is to provide a **proof-of-concept**. We experiment on the commonly used Purchase-100 [40], CelebA [28], CIFAR-10 [25] and AG News [49] datasets. We will describe the details of how we split the dataset, train models, construct ranges, and obtain samples in Section 5.1. Since the range membership notion is new, we do not have a prior method to compare with. However, since the goal of introducing this new privacy notion is to enable better and more comprehensive privacy auditing, we compare RaMIA with the de-factor privacy auditing framework, MIA. We show that RaMIA performs better (Sec 5.5) in scenarios where MIA under-performs (Depicted in Figure 2). Both MIA and RaMIA in the experiments are built upon the state-of-the-art attack algorithm, robust membership inference attack (RMIA) [48], with a few reference models trained in the same way as [5] and [48]. The respective queries are outlined in Table 1, and the definitions of members under each attack framework are explained in Table 2. In both tables, x represents original data in datasets, while x' s are either data with missing values or modified data from x . The reason that we do not test our attacks by taking ranges centered at original data x is that the chance of the attack data being exactly the same

Table 1: Range queries and point queries used in our experiments for RaMIA and MIA respectively.

Dataset	Range query	Point query
Purchase-100	possible data records given the incomplete data x'	mode imputed x'
CelebA	photos featuring the same person as photo x'	photo x'
CIFAR-10	transformed versions of image x'	image x'
AG News	sentences that are of Hamming distance 8 to sentence x'	sentence x'

Table 2: Definitions of range and point members corresponding to the attack queries in Table 1.

Dataset	Range member if there is at least	(Point) member if
Purchase-100	one training point matches with x' on all unmasked columns	x'_{impu} is member
CelebA	one training image featuring the same person as x'	x' is member
CIFAR-10	one version of image x' in the training set	x' is member
AG News	one training sentence within Hamming distance 8 to x'	x' is member

as the training data is extremely low without sufficient prior knowledge. It is more realistic that similar data are being queried.

5.1 Setup details

As mentioned earlier, the range function must come from the semantics of privacy. Hence, in experiments, we use specific range functions with different data types. For tabular data, we consider missing columns, which is an extreme case of using Euclidean distance on missing columns as a range function. For human photo data, we use a semantic range function, which is based on the main person featured in the photo. For other image data, we use geometric transformations as range functions. For text data, we use (word level) Hamming distance, which is edit distance or Levenshtein distance that only considers word substitution. The reasons for choosing these range functions have been motivated and explained in earlier parts of this paper.

5.1.1 Tabular data: Purchase-100

- **Dataset** Purchase-100 [40] is a tabular dataset derived from Kaggle’s Acquire Valued Shoppers Challenge ¹. This dataset was first curated by [40] such that there are 600 binary features, each representing if each person, represented by each row, has purchased the product. The data is then divided into 100 classes, and the task is to predict the category of the person given the purchase history.
- **Models** We train five-layer multi-layer perceptron (MLP) models in PyTorch [34] on half of the entire dataset. The hidden layers are of sizes [512, 256, 128, 64], identical to the setup in [48]. All models achieve a test accuracy of 83%.
- **Construction of ranges** We simulate the scenario where the attacker has incomplete data (data with missing values). For all training and test data records, we randomly mask k columns. Each row with masked columns is a range query that contains 2^k possible

¹<https://www.kaggle.com/c/acquire-valued-shoppers-challenge/data>

points as each feature is binary. We then check if each range constructed from test data points includes any training point. If so, they are re-labeled as "IN-ranges".

- **Sampling within ranges** Since this dataset contains 600 independent binary features, we do Bernoulli sampling independently for all missing columns. The parameter of the sampler is computed by taking the average value of each column. Because of the nature of this dataset, our sampled data can be regarded as in-distribution. We take 19 samples for each range, together with the data obtained by doing mode imputation (fill in the missing values with the modes).

5.1.2 Image data I: CelebA

- **Dataset** CelebA [28], also known as the CelebFaces Attributes dataset, contains 202,599 face images from 10,177 celebrities, each annotated with 40 binary facial features. We construct the members set by only including photos of celebrities with identity numbers smaller than 5090. The rest are used to construct the non-members set. For each celebrity in the members set, half of the photos are put into the training set, while the other half goes into the holdout set.
- **Models** We train four-layer convolutional neural networks (CNNs) in PyTorch [34] on the training set to predict the facial attributes of any given photo. Our target model has a test accuracy of 87%.
- **Construction of ranges** The range function here is a semantic one that is based on the identity of the face image. For example, a range query can be "all Alice's photos". Since the identities in the training and non-members set are disjoint, it is easy to construct IN- and OUT-ranges based on the distribution of identities in the two sets.
- **Sampling within ranges** For each range query, we curate all images in the holdout set that share the same identity as the range center to construct our sample set.

5.1.3 Image data II: CIFAR-10

- **Dataset** CIFAR-10 [25] is a popular image classification dataset. There are 50,000 training images, each of size (32, 32, 3).
- **Models** We train WideResNets-28-2 [47] with JAX [2] on half of the training set of CIFAR-10 using the code from [5], with and without image augmentations. Our target model trained without augmentation achieves a test accuracy of 83% on the CIFAR-10 test set, and the target model trained with augmentation achieves a test accuracy of 92%. The train time augmentation is the composition of random flipping, cropping and random hue.
- **Construction of ranges** The range function here is different types of image augmentations, which are geometric transformations. An example of a range query is "all transformed version of image X ". For each training and test image, a range is constructed by applying different transformations.
- **Sampling within ranges** For each range query, we independently apply 15 image augmentations on the query center. The augmentations include flipping, random rotation,

random resizing and cropping, random contrast, brightness, hue, and the composition of them.

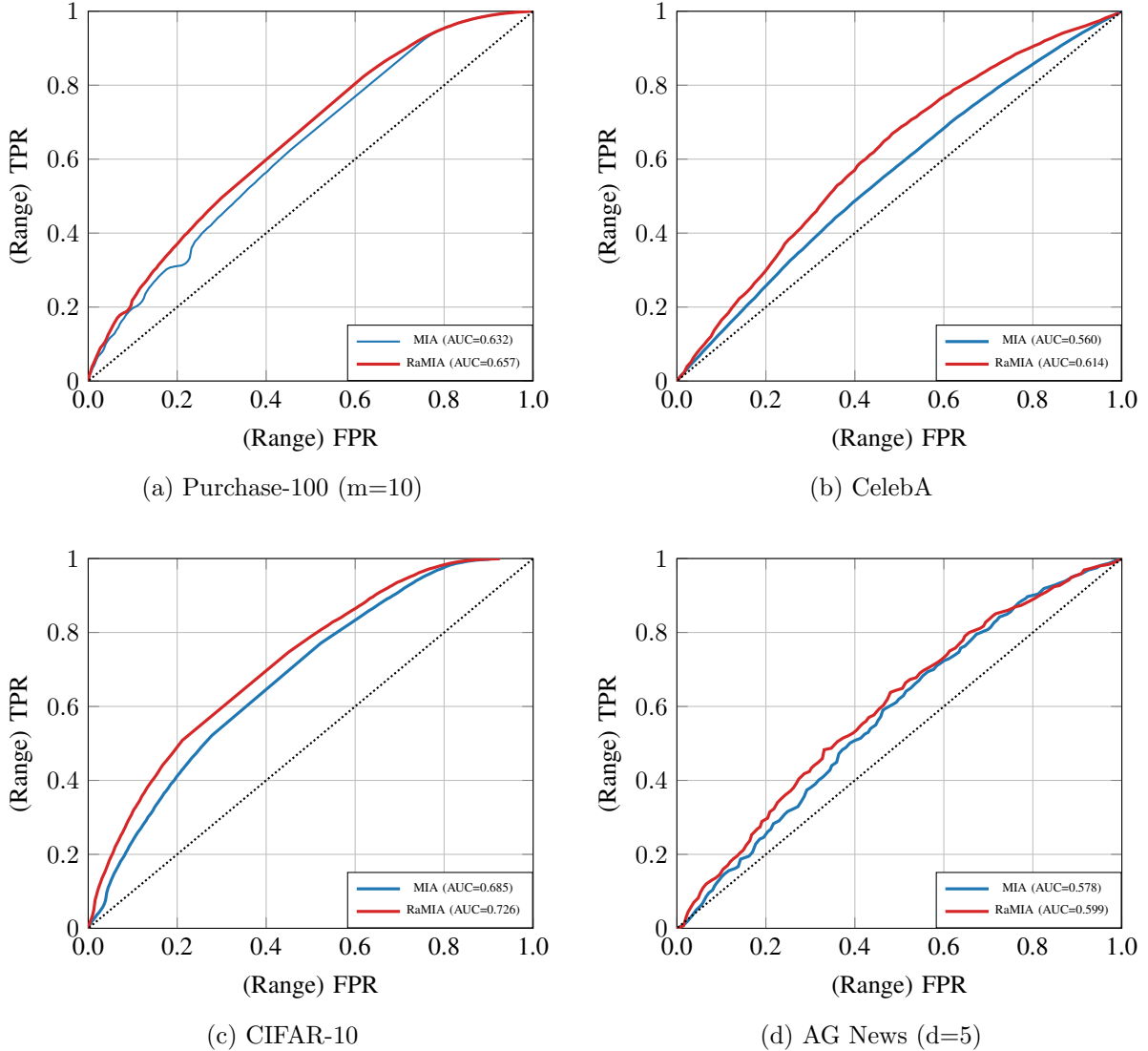


Figure 3: RaMIA performs better than MIA on points that are close to original points but not exactly the same.

5.1.4 Textual data: AG News

- **Dataset** We use the AG News dataset [49], which is a news collection with four categories of news. Although it was introduced as a text classification dataset, we disregard the labels and treat it as a text generation dataset. There are 120,000 sentences in its training set. It is a popular text dataset in LLM MIA literature [33].
- **Models** We took pretrained GPT-2 [35] models from Hugging Face’s transformers library, and finetuned them on half of AG News’ training set with LoRA [19] implemented in

Hugging Face’s PEFT [32] library. The finetuning is done for 4 epochs. Our target model achieves a perplexity of 1.39 on the test set of AG News.

- **Construction of ranges** The range function here is word-level Hamming distance, which can be thought of as the edit distance measured on word level that only allows word substitution. An example of a range query is ”all sentences within Hamming distance d to sentence x ”. To construct IN- and OUT-ranges, we just need to specify the max Hamming distance and the starting sentence. We constructed the starting sentences by randomly masking α words from the training and test sentences, before filling in the mask with a pretrained BERT [12] model, so they have a distance of α to the original training/test sentences. A Hamming distance is then specified with each starting sentence to form a range.
- **Sampling within ranges** We mask the range center by k words where k is the Hamming distance specified by the range. Then we use BERT [12] to replace the mask with one of the top choices.

5.2 Hyperparameters

Overall, on Purchase-100, we take 20 samples in every range, and set $q_e = 100, q_s = 45$. On CIFAR-10, we apply up to 15 distinct transforms, and set $q_e = 100, q_s = 40$. On AG News, we construct 50 sentences within each range, and set $q_e = 100, q_s = 20$. On CelebA, each celebrity has a different number of images in the sampling space, ranging from 1 to 18. Since it is hard to standardize the sample size for all ranges, we take all of them. We then set $q_s = 0$ and $q_e = 25$, which means we are not trimming anything for ranges with very few samples available.

5.3 Implementation details

We train 8 models on Purchase-100 and CIFAR-10, and train 4 models on CelebA and AG News. Each model is trained on half of the dataset, as described in [5, 48]. For all PyTorch models, we use Adam as our optimizer with a learning rate of 0.001. For WideResnets, we use the training code from [5]. On AG News, the models are trained for 4 epochs. On other datasets, they are trained for 100 epochs. All training is done on two Nvidia RTX 3090 GPUs. Training on AG News takes about 1 hour per epoch. Training other models takes less than one hour each.

5.4 Metrics

To evaluate the performance of RaMIA and MIA based on the same MIA algorithm, we use AUCs. The inputs to RaMIA are range queries in Table 1, while the inputs to MIA are point queries, which are range centers, in Table 1. The ground truth membership for both RaMIA and MIA is the range membership information defined in Table 2, which allows us to compare the power of both inference attack frameworks in identifying queries that are privacy leaking. In other words, both point and range TPRs/FPRs are calculated against the range membership information. Following [5], we also report (Range) TPR at small (Range) FPR for both MIA and RaMIA (Table 4).

5.5 RaMIAs quantify privacy risks more comprehensively than MIAs

As we have explained before, data points that are close enough to the training data are out of the scope of membership inference attacks. We observe from Figure 3 that range membership inference attacks are better at identifying those nearby points, and thus providing more comprehensive privacy auditing on all the four datasets we tested. We want to emphasize that the gain is remarkable if we consider how little samples were taken compared to the range sizes. On Purchase-100, there are a total of 1024 candidates, and we take less than 20% of them. On AG News, there are millions of sentences within a distance of 8. 50 sentences are too little to meaningfully cover anything in the space. Yet, limited samples can lead to noticeable gains, which further shows the current privacy quantification approach is suboptimal and needs a better framework. Due to randomness in sampling, we report the average gain of RaMIA over MIA with standard deviation in Table 3. TPRs at small FPRs are in Table 4. The improvement in AUC is summarized in Table 3.

Table 3: Improvement in AUCs after switching from MIA to RaMIA across multiple iterations of random sampling. We do not randomly sample but use all available attack images in CelebA.

	Purchase-100	CIFAR-10	CelebA	AG News
ΔAUC	2.62 ± 0.04	4.12 ± 0.06	5.4	1.20 ± 0.2

Relation to user-level inference Note that in the CelebA experiment, we use identify information as the semantic range function, making it similar to user-level inference. This further shows that RaMIA is a better and more comprehensive privacy auditing framework. In terms of algorithms, our attack strategy should dominate the simple averaging approach used in prior work [31, 23], since the trimming ratio is optimized (compared to no trimming in simple averaging). There are other user-level inference algorithms [11] that train additional shadow models and classifiers, which incurs additional computational costs. They also consider scenarios where user information is the label of their target models, e.g. facial and speech recognition systems that predict user ID as their outputs [11, 10]. This encourages their target models to explicitly cluster data based on user information, making inference easier. On the other hand, our target model, a facial attribute classifier, does not use user information anywhere in the training, making the inference harder.

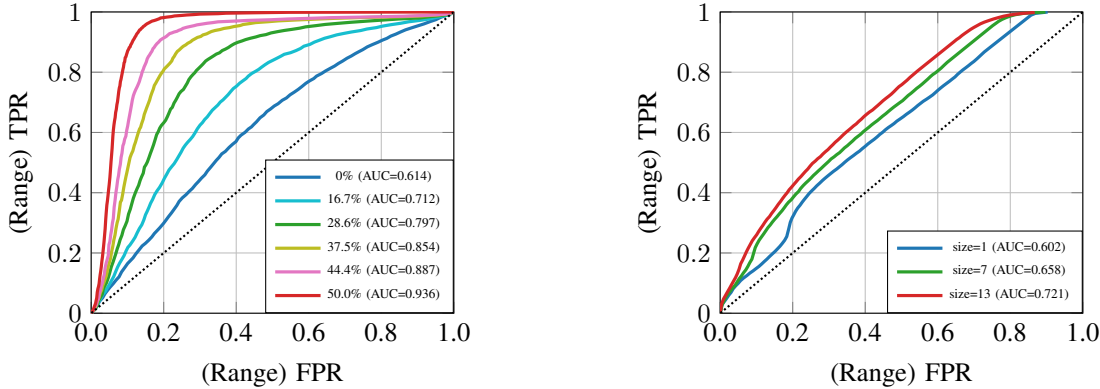
5.6 Factors affecting RaMIA performance

Training data density in the range Due to the nature of the sampling-based approach, the chance of our attack set containing a true training point scales linearly with the density of training points in the range. If we keep the sample size constant, increasing the range without including more training points in the range hurts the attack performance because the chance of the attack set including any training point gets diluted. On the other hand, if we increase the training point density, which is equivalent to increasing the probability the attacker samples a true training point, the attack performance gets boosted. Figure 4b shows that the performance of RaMIA increases when the range becomes larger in the CIFAR-10 experiment. Recall that the range function in CIFAR-10 is based on image augmentation methods. Increasing the range means the attacker applies more distinct augmentation methods to obtain transformed images.

Table 4: True Positive Rate under different attacks on different datasets at small false positive rates of 1% and 0.1%. MIAs cannot be conducted on incomplete data, so we fill the missing columns with the modes and run the attack on them. Standard deviation over random sampling iterations is reported, except for CelebA, where we use all available candidates. The TPR and FPR are calculated based on the range membership information, as described in Sec 5.4. For a fair comparison, we should compare RaMIA and MIA based on the same membership testing backbone, e.g. MIA with RMIA versus RaMIA with RMIA.

TPR@FPR(%)	Purchase-100		CIFAR-10		CelebA		AG News	
	1%	0.1%	1%	0.1%	1%	0.1%	1%	0.1%
MIA								
LOSS	0	0	0.15	0	1.86	0.31	0.08	0
RMIA	2.18	0.37	2.40	0.21	1.69	0.19	0.30	0
RaMIA								
LOSS	0 ± 0	0 ± 0	1.17 ± 0.06	0.05 ± 0.03	1.40	0.28	1.10 ± 0.11	0 ± 0
RMIA	2.57 ± 1.58	0.57 ± 0.47	3.59 ± 0.11	0.80 ± 0.02	1.44	0.22	0.54 ± 0.12	0 ± 0

This increases the chance of the attacker obtaining one of the transformed versions of training images seen by the model during training, thus leading to better attack performance. In Figure 3b, we conducted the attack assuming the attacker cannot sample any true training images. As a sanity check, we relax this assumption, and Figure 4a shows that RaMIA performs monotonically better when the density of training images increases from 0% to 50%, when the number of samples is constant.



(a) RaMIA on CelebA gets better when the training points available for sampling increases. The percentages are the density of training points in the distribution that the attack samples from. (Sanity Check)

(b) RaMIA performs better on CIFAR-10 when the range size increases. The range size here is equal to the number of distinct transformations applied to images.

Figure 4: Attack performance increases in tandem with training point density.

Susceptibility to MIAs and RaMIAs is correlated Ranges containing training points that are susceptible to MIAs are also more susceptible to RaMIAs. Researchers have previously

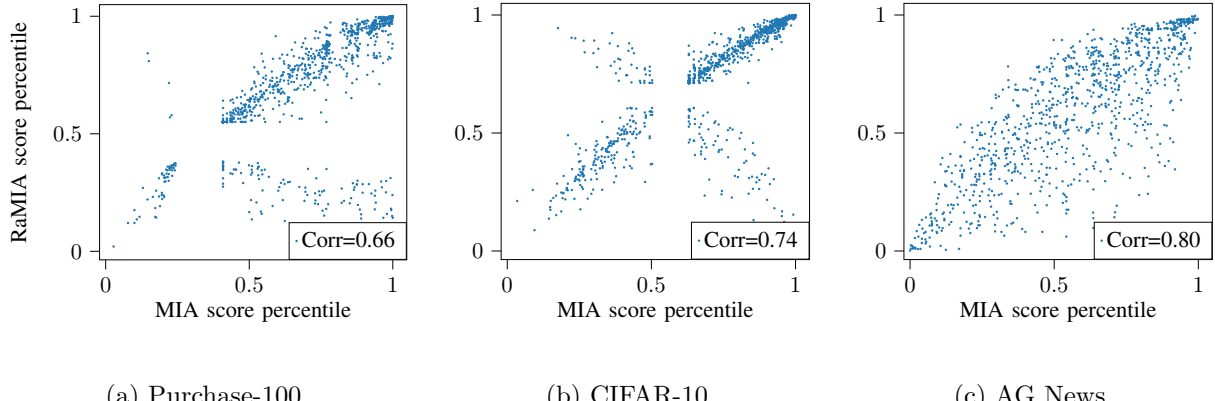


Figure 5: Correlation between the percentile of RaMIA and MIA scores of members among non-members. The larger the percentile is, the more non-members the member dominates, and the more likely for it to be classified as IN. The Pearson correlation coefficients are provided for each plot. It shows that the vulnerability to MIA is positively correlated with that to RaMIA.

discovered that machine learning models memorize duplicate data more [26, 6]. In our CelebA dataset, each celebrity has a different number of photos in the training set, which can be thought of as each identity having different levels of duplication in the training set. Similar to the insights from MIAs, we also observe that identities that have more training images, i.e. higher duplication rate, are more susceptible to RaMIA. Figure 6 shows the relationship between the percentile of each range’s RaMIA score within non-members’ RaMIA scores and the duplication rate. Generally speaking, identities that have more training photos are more prone to RaMIAs. Similarly, correlation can be observed on the other three datasets in our experiments, where the training points’ RaMIA score percentiles among non-members are positively correlated with their MIA score percentiles 5.



Figure 6: Number of photos from the same celebrity in the training set affects the identifiability of the range.

5.7 Mismatched training and attack data hurts attack performance

Figure 2c shows that MIA underestimates the privacy risk when the augmentation used in training and attacking differs. This rings a bell as many people audit the privacy risk of image classifiers with original images, when the classifiers are often trained with a composition of augmentations. Many transformations, such as color jittering and affine transformations, always produce different final images. Other commonly used augmentation methods, such as random cropping, introduce more randomness to the pipeline. Hence, it is almost certain that the original images are never seen by the model. Therefore, we should use RaMIA for a better auditing result (Figure 3c).

Difference to existing augmentation-based MIAs Existing attacks [5, 48] also use augmented queries in the attack, but with a different rationale and assumption of the attacker’s knowledge. Since they adopt the existing privacy notion based on point queries, only (augmented) images seen by the model in the training stage are considered as members. Hence, the attacker needs to know the exact train-time augmentations and augment images accordingly to not violate the privacy notion. In RaMIA, the set of augmentations is given by the challenger (Def 2), which can contain augmentations not used in training, but considered as privacy leaking. Using the aggregation method in [5] will hurt the attack performance if non-training augmentations are used. However, RaMIA is designed to be robust in this scenario (Fig 3c) due to its trimming process.

5.8 RaMIA on redacted data

Many large language models (LLMs) are trained with sensitive textual data. Some of the data with sensitive information redacted might be publicly available. Similar to our experiment with data with missing values, we can apply RaMIA to redacted data to identify which of them are used to train a target LLM. Accurately identifying the redacted sentences paves the way for reconstructing them as a follow-up attack. Figure 7 shows the results. In this experiment, we use spaCy [18] to mask peoples’ names to simulate the masking of personally identifiable information (PII). We then generate 10 possible sentences for each masked sentence using BERT and conduct RaMIA. The MIA performance is the average attack performance over all 10 possible sentences. The performance gap is smaller compared to that in Figure 3d. The reason might be that BERT fails to produce diverse PII completions, making all candidate sentences similar to each other, and reducing the power of RaMIA.

6 Conclusion

In this paper, we argue that membership inference attacks are only useful as a privacy audit tool when querying exact copies of training and test data. Moving the query to similar points causes a drastic decrease in performance, rendering MIAs less useful. We conclude MIAs fail to comprehensively capture the notion of privacy, and thus propose a new class of inference attack, RaMIA, that extends the notion of MIAs and covers the failure cases of MIAs by checking if a given range contains a training point. We introduce RaMIA as an attack framework that can be implemented with any existing MIA algorithm. We show that it can provide better privacy auditing with very few samples taken randomly. We hope our work can make more privacy researchers and practitioners aware of the shortcomings of MIAs, and shift their attention to

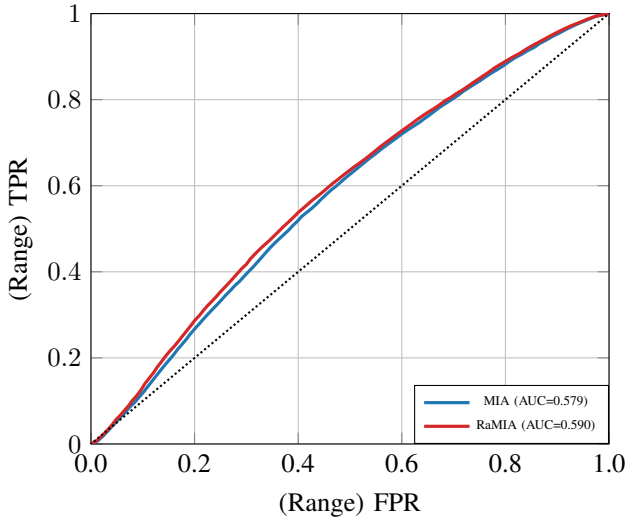


Figure 7: RaMIA on a subset of AG News where names are redacted.

RaMIA. As it is the first paper that brings up this new framework, there is room for improvement in specific attack algorithms. For example, a better sampling process will surely increase the gap between RaMIA and MIA. Nevertheless, we have shown our framework is sensible and useful. In future work, we hope to design more powerful RaMIA strategies that are robust to the change of membership signals and datasets, especially on LLMs where we believe our privacy notion is extremely relevant.

References

- [1] G. Ateniese, L. V. Mancini, A. Spognardi, A. Villani, D. Vitali, and G. Felici. Hacking smart machines with smarter ones: How to extract meaningful data from machine learning classifiers. *International Journal of Security and Networks*, 10(3):137–150, 2015.
- [2] J. Bradbury, R. Frostig, P. Hawkins, M. J. Johnson, C. Leary, D. Maclaurin, G. Nuclea, A. Paszke, J. VanderPlas, S. Wanderman-Milne, and Q. Zhang. JAX: composable transformations of Python+NumPy programs, 2018. URL <http://github.com/google/jax>.
- [3] G. Brown, M. Bun, V. Feldman, A. Smith, and K. Talwar. When is memorization of irrelevant training data necessary for high-accuracy learning? In *Proceedings of the 53rd annual ACM SIGACT symposium on theory of computing*, pages 123–132, 2021.
- [4] N. Carlini, F. Tramer, E. Wallace, M. Jagielski, A. Herbert-Voss, K. Lee, A. Roberts, T. Brown, D. Song, U. Erlingsson, et al. Extracting training data from large language models. In *30th USENIX Security Symposium (USENIX Security 21)*, pages 2633–2650, 2021.
- [5] N. Carlini, S. Chien, M. Nasr, S. Song, A. Terzis, and F. Tramer. Membership inference attacks from first principles. In *2022 IEEE Symposium on Security and Privacy (SP)*, pages 1897–1914. IEEE, 2022.

- [6] N. Carlini, D. Ippolito, M. Jagielski, K. Lee, F. Tramer, and C. Zhang. Quantifying memorization across neural language models. *arXiv preprint arXiv:2202.07646*, 2022.
- [7] N. Carlini, J. Hayes, M. Nasr, M. Jagielski, V. Sehwag, F. Tramer, B. Balle, D. Ippolito, and E. Wallace. Extracting training data from diffusion models. In *32nd USENIX Security Symposium (USENIX Security 23)*, pages 5253–5270, 2023.
- [8] M. Chase, E. Ghosh, and S. Mahloujifar. Property inference from poisoning. *arXiv preprint arXiv:2101.11073*, 2021.
- [9] H. Chaudhari, J. Abascal, A. Oprea, M. Jagielski, F. Tramer, and J. Ullman. Snap: Efficient extraction of private properties with poisoning. In *2023 IEEE Symposium on Security and Privacy (SP)*, pages 400–417. IEEE, 2023.
- [10] G. Chen, Y. Zhang, and F. Song. Slmia-sr: Speaker-level membership inference attacks against speaker recognition systems. *arXiv preprint arXiv:2309.07983*, 2023.
- [11] M. Chen, Z. Zhang, T. Wang, M. Backes, and Y. Zhang. {FACE-AUDITOR}: Data auditing in facial recognition systems. In *32nd USENIX Security Symposium (USENIX Security 23)*, pages 7195–7212, 2023.
- [12] J. Devlin, M.-W. Chang, K. Lee, and K. Toutanova. Bert: Pre-training of deep bidirectional transformers for language understanding. *arXiv preprint arXiv:1810.04805*, 2018.
- [13] M. Duan, A. Suri, N. Mireshghallah, S. Min, W. Shi, L. Zettlemoyer, Y. Tsvetkov, Y. Choi, D. Evans, and H. Hajishirzi. Do membership inference attacks work on large language models? *arXiv preprint arXiv:2402.07841*, 2024.
- [14] V. Feldman. Does learning require memorization? a short tale about a long tail. corr abs/1906.05271 (2019). *arXiv preprint arXiv:1906.05271*, 2019.
- [15] V. Feldman and C. Zhang. What neural networks memorize and why: Discovering the long tail via influence estimation. *Advances in Neural Information Processing Systems*, 33: 2881–2891, 2020.
- [16] I. Garg and K. Roy. Memorization through the lens of curvature of loss function around samples. *arXiv preprint arXiv:2307.05831*, 2023.
- [17] B. Hilprecht, M. Härterich, and D. Bernau. Monte carlo and reconstruction membership inference attacks against generative models. *Proceedings on Privacy Enhancing Technologies*, 2019.
- [18] M. Honnibal, I. Montani, S. Van Landeghem, and A. Boyd. spaCy: Industrial-strength Natural Language Processing in Python. 2020. doi: 10.5281/zenodo.1212303.
- [19] E. J. Hu, P. Wallis, Z. Allen-Zhu, Y. Li, S. Wang, L. Wang, W. Chen, et al. Lora: Low-rank adaptation of large language models. In *International Conference on Learning Representations*, 2021.
- [20] B. Jayaraman and D. Evans. Are attribute inference attacks just imputation? In *Proceedings of the 2022 ACM SIGSAC Conference on Computer and Communications Security*, pages 1569–1582, 2022.

- [21] B. Jayaraman, L. Wang, K. Knipmeyer, Q. Gu, and D. Evans. Revisiting membership inference under realistic assumptions. *Proceedings on Privacy Enhancing Technologies*, 2021 (2), 2021.
- [22] H. Jeffreys. Theory of probability. 1939.
- [23] N. Kandpal, K. Pillutla, A. Oprea, P. Kairouz, C. A. Choquette-Choo, and Z. Xu. User inference attacks on large language models. *arXiv preprint arXiv:2310.09266*, 2023.
- [24] Y. I. Kim, P. Agrawal, J. O. Royset, and R. Khanna. On memorization and privacy risks of sharpness aware minimization. *arXiv preprint arXiv:2310.00488*, 2023.
- [25] A. Krizhevsky et al. Learning multiple layers of features from tiny images. 2009.
- [26] K. Lee, D. Ippolito, A. Nystrom, C. Zhang, D. Eck, C. Callison-Burch, and N. Carlini. Deduplicating training data makes language models better. *arXiv preprint arXiv:2107.06499*, 2021.
- [27] F. Liu, T. Lin, and M. Jaggi. Understanding memorization from the perspective of optimization via efficient influence estimation. *arXiv preprint arXiv:2112.08798*, 2021.
- [28] Z. Liu, P. Luo, X. Wang, and X. Tang. Large-scale celebfaces attributes (celeba) dataset. *Retrieved August, 15(2018):11*, 2018.
- [29] Y. Long, Z. Ying, H. Yan, R. Fang, X. Li, Y. Wang, and Z. Pan. Membership reconstruction attack in deep neural networks. *Information Sciences*, 634:27–41, 2023.
- [30] M. Lukasik, V. Nagarajan, A. S. Rawat, A. K. Menon, and S. Kumar. What do larger image classifiers memorise? *arXiv preprint arXiv:2310.05337*, 2023.
- [31] S. Mahloujifar, H. A. Inan, M. Chase, E. Ghosh, and M. Hasegawa. Membership inference on word embedding and beyond. *arXiv preprint arXiv:2106.11384*, 2021.
- [32] S. Mangrulkar, S. Gugger, L. Debut, Y. Belkada, S. Paul, and B. Bossan. Peft: State-of-the-art parameter-efficient fine-tuning methods. <https://github.com/huggingface/peft>, 2022.
- [33] J. Mattern, F. Mireshghallah, Z. Jin, B. Schoelkopf, M. Sachan, and T. Berg-Kirkpatrick. Membership inference attacks against language models via neighbourhood comparison. In *Findings of the Association for Computational Linguistics: ACL 2023*, pages 11330–11343, 2023.
- [34] A. Paszke, S. Gross, F. Massa, A. Lerer, J. Bradbury, G. Chanan, T. Killeen, Z. Lin, N. Gimelshein, L. Antiga, et al. Pytorch: An imperative style, high-performance deep learning library. *Advances in neural information processing systems*, 32, 2019.
- [35] A. Radford, J. Wu, R. Child, D. Luan, D. Amodei, I. Sutskever, et al. Language models are unsupervised multitask learners. *OpenAI blog*, 1(8):9, 2019.
- [36] A. Sablayrolles, M. Douze, C. Schmid, Y. Ollivier, and H. Jégou. White-box vs black-box: Bayes optimal strategies for membership inference. In *Proceedings of the 36th International Conference on Machine Learning (ICML '19)*, page 5558–5567, 2019.

- [37] A. Salem, A. Bhattacharya, M. Backes, M. Fritz, and Y. Zhang. {Updates-Leak}: Data set inference and reconstruction attacks in online learning. In *29th USENIX security symposium (USENIX Security 20)*, pages 1291–1308, 2020.
- [38] P. Samarati and L. Sweeney. Generalizing data to provide anonymity when disclosing information. In *PODS*, volume 98, pages 10–1145, 1998.
- [39] S. Sankararaman, G. Obozinski, M. I. Jordan, and E. Halperin. Genomic privacy and limits of individual detection in a pool. *Nature genetics*, 41(9):965–967, 2009.
- [40] R. Shokri, M. Stronati, C. Song, and V. Shmatikov. Membership inference attacks against machine learning models (s&p’17). 2017.
- [41] A. Suri and D. Evans. Formalizing and estimating distribution inference risks. *Proceedings on Privacy Enhancing Technologies*, 2022.
- [42] K. Tirumala, A. Markosyan, L. Zettlemoyer, and A. Aghajanyan. Memorization without overfitting: Analyzing the training dynamics of large language models. *Advances in Neural Information Processing Systems*, 35:38274–38290, 2022.
- [43] H. Van Trees. Detection, estimation, and modulation theory. part 1-detection, estimation, and linear modulation theory. 1968.
- [44] Y. Wu, N. Yu, Z. Li, M. Backes, and Y. Zhang. Membership inference attacks against text-to-image generation models. 2022.
- [45] J. Ye, A. Maddi, S. K. Murakonda, V. Bindschaedler, and R. Shokri. Enhanced membership inference attacks against machine learning models. In *Proceedings of the 2022 ACM SIGSAC Conference on Computer and Communications Security*, pages 3093–3106, 2022.
- [46] S. Yeom, I. Giacomelli, M. Fredrikson, and S. Jha. Privacy risk in machine learning: Analyzing the connection to overfitting. In *2018 IEEE 31st computer security foundations symposium (CSF)*, pages 268–282. IEEE, 2018.
- [47] S. Zagoruyko and N. Komodakis. Wide residual networks. In *British Machine Vision Conference 2016*. British Machine Vision Association, 2016.
- [48] S. Zarifzadeh, P. C.-J. M. Liu, and R. Shokri. Low-cost high-power membership inference by boosting relativity. 2023.
- [49] X. Zhang, J. Zhao, and Y. LeCun. Character-level convolutional networks for text classification. *Advances in neural information processing systems*, 28, 2015.

A Attack algorithms

In this section, we explain the details of the membership inference attack algorithms used in our experiments.

LOSS LOSS [46] computes loss values as a proxy of membership score on given points: $MIA(x; \theta) = l(x; \theta)$. To compute the likelihood, an easy way is to take the exponential of the negative of the loss $\mathbb{P} = \exp^{-l}$.

RMIA RMIA [48] computes membership score by applying chain rule: $\mathbb{P}(\theta|x) = \frac{\mathbb{P}(x|\theta)\mathbb{P}(\theta)}{\mathbb{P}(x)}$. The score is then compared with all available population data points to obtain the percentage of population points being dominated by the given point: $\mathbb{P}_{z \in Z}[\frac{\mathbb{P}(\theta|x)}{\mathbb{P}(\theta|z)} \geq \gamma]$, where the term $\mathbb{P}(\theta)$ will cancel out with each other. The normalizing constant $\mathbb{P}(x)$ is computed with reference models: $\mathbb{P}(x) = 0.5\mathbb{E}_{\theta_{\text{IN}}}\mathbb{P}(x|\theta_{\text{IN}}) + 0.5\mathbb{E}_{\theta_{\text{OUT}}}\mathbb{P}(x|\theta_{\text{OUT}})$. In its offline version, the in models are unavailable. In this case, the former probabilities are approximated by the latter term $\mathbb{P}_{\text{IN}} = a\mathbb{P}_{\text{OUT}} + (1 - a)$. The hyperparameter α is chosen based on the reference models. Specifically, one reference model is chosen as the temporary target model, and the rest are used to attack it. The value of α is chosen to be the best-performing value under this setting, obtained via a simple sweeping. In our experiment, we use the offline attack only. The α values for Purchase-100 and CIFAR-10 are taken from [48]. For CelebA, we set it to be 0.33. For AG News, we set it to be 1.0.